# Butorphanol inhibits ferroptosis to attenuate PC12 cell injury by blocking JNK/p38 signaling

LULU JI, QING SHE, PING ZHOU and YIBIN QIN

Department of Anesthesiology, Affiliated Hospital of Nantong University, Nantong, Jiangsu 226001, P.R. China

Received April 6, 2023; Accepted August 16, 2023

DOI: 10.3892/etm.2023.12295

**Abstract.** Butorphanol is a synthetic selective opioid receptor antagonist that exhibits substantial analgesic effects. The present study aimed to explore the effects of butorphanol on a neurodegenerative disease cell model and to investigate its specific regulatory mechanism. Cell viability of PC12 cells was assessed using the Cell Counting Kit-8 assay. Oxidative stress levels were measured by the corresponding kits and western blotting of specific protein markers. Apoptosis was determined using the terminal-deoxynucleoitidyl transferase mediated nick end labeling assay and by western blotting. Western blotting was used to analyze the expression levels of c-Jun NH2-terminal kinase (JNK)/p38 signaling pathway-related proteins. Thiobarbituric acid-reactive substances and $Fe^{+2}$ content were detected using the corresponding assay kits and the expression levels of ferroptosis-associated proteins were assessed by western blotting following the addition of the JNK activator anisomycin (ANI). Oxidative stress and apoptosis were examined with the aforementioned assays following the supplementation of ANI or the ferroptosis inducer erastin (ERA). It was revealed that butorphanol dose-dependently enhanced the viability and suppressed the oxidative stress and apoptosis of $H_2O_2$-treated PC12 cells. In addition, butorphanol blocked JNK/p38 signaling and hampered ferroptosis, while this effect was reversed by ANI. ANI or ERA reversed the effects of butorphanol on oxidative stress and apoptosis of $H_2O_2$-treated PC12 cells. In summary, butorphanol suppressed ferroptosis by blocking JNK/p38 signaling to impart inhibitory effects on oxidative stress and apoptosis in a neurodegenerative disease cell model.

## Introduction

Butorphanol is an opioid agonist-antagonist that exhibits protective effects on specific organs, such as the brain, the lungs and the heart (1). The potential mechanism of action of butorphanol depends on the dual pharmacological functions of κ-opioid and $\mu$-receptors activated by specific metabolites (2). It has been acknowledged that butorphanol can be administered via different routes, such as intravenous administration, intramuscular injection and nasal spray (3). Previous studies have shown that butorphanol is widely applied in clinical practice. For example, as a synthetic opioid, butorphanol has been reported to inhibit tumor growth and metastasis as well as inflammation, oxidative stress and apoptosis in cerebrovascular diseases (3,4). However, the neuroprotective effects of butorphanol on neurodegenerative diseases have not yet been determined.

Neurodegenerative diseases comprise several biological events, including oxidative stress and programmed cell death (5). Ferroptosis is a novel iron-dependent process of programmed cell death featured by excessive accumulation of lipid peroxides and reactive oxygen species (6). Emerging evidence has supported that ferroptosis is closely implicated in the process of neurodegenerative diseases (7). Hydrogen peroxide ($H_2O_2$) is often used to establish the model of oxidative damage due to its strong oxidant properties (8,9). In brain cells, $H_2O_2$ acts as an intracellular regulator of neuronal activity, growth and organelle function as well as a diffusible messenger of neuron-glia signaling and interneuronal communication, including the regulation of synaptic transmission and plasticity (10). To effectively clarify the effects of butorphanol on neurodegenerative diseases, $H_2O_2$ was used to treat PC12 cells so as to establish an *in vitro* model of oxidative damage.

Among the kinases, mitogen-activated protein kinase (MAPK) plays an indispensable role in neurodegeneration (11). The c-Jun NH2-terminal kinase (JNK) and the p38 MAP kinase, belong to the MAPK family of enzymes and are responsible for stress signaling and pro-inflammatory cytokine stimulation (12). The transit of upstream signals to downstream factors during the activation of the JNK/p38 MAPK may mediate apoptosis, differentiation, growth or immune responses (13-15). Furthermore, the tight correlation between ferroptosis and JNK signaling has also been highlighted (16,17). In addition, the inhibition of JNK and MAPK enzymes can prevent neural damage (18).

The purpose of the present study was to identify the role of butorphanol in the prevention of neurodegenerative disease cell model, and the mechanism of action of the association between butorphanol and the JNK/p38 signaling pathway.

*Correspondence to:* Dr Yibin Qin, Department of Anesthesiology, Affiliated Hospital of Nantong University, 20 Xisi Road, Chongchuan, Nantong, Jiangsu 226001, P.R. China
E-mail: qybtougao@163.com

*Key words:* butorphanol, ferroptosis, oxidative stress, JNK/p38 signaling

The present study may offer a novel strategy for the study of neurodegenerative diseases.

## Materials and methods

*Cell culture and treatment*. PC12 cells were obtained from BeNa Culture Collection. The cells were incubated with DMEM supplemented with 10% FBS (Thermo Fisher Scientific, Inc.), 100 U/ml penicillin, and 100 $\mu$g/ml streptomycin in a humid environment at 37˚C with 5% $CO_2$. PC12 cells were incubated in 96-well plates for 24 h. Subsequently, 400 $\mu$M $H_2O_2$ was incubated with the cells for 1 h at room temperature so as to establish an *in vitro* cell injury model. Following the indicated treatment, PC12 cells were incubated with butorphanol at different doses (1, 2 and 4 $\mu$M) for 24 h and a series of cellular experiments were conducted to investigate the effects of butorphanol on $H_2O_2$-induced PC12 cell injury.

*Cell Counting Kit-8 (CCK-8)*. PC12 cells were incubated in 96-well plates, at a density of $5x10^3$, for 24 h. Subsequently, 10 $\mu$l CCK-8 reagent (Beyotime Institute of Biotechnology) was added to each well and the plate was incubated for an additional 2 h. The absorbance was detected at a wavelength of λ=450 nm using a microplate reader (Molecular Devices, LLC), and cell viability was expressed as the ratio of the measured wavelength to the control wavelength.

*Detection of oxidative stress*. The lysis of PC12 cells was performed by cell lysis buffer (Beyotime Institute of Biotechnology; cat. no. P0013). Subsequently, the cells were centrifuged at 10,000 x g for 10 min at 4˚C and 200 $\mu$l supernatant was collected. Malondialdehyde (MDA; cat. no. S0131S), superoxide dismutase (SOD; cat. no. S0088), glutathione peroxidase (GSH-Px; cat. no. S0056) and catalase (CAT; cat. no. S0082) (Beyotime Institute of Biotechnology) assay kits were used to determine the contents of MDA, SOD, GSH-Px, and CAT, separately.

*Western blotting*. PC12 cells were isolated using RIPA lysis buffer (Beyotime Institute of Biotechnology; cat. no. P0013B) and quantified by the bicinchoninic acid protein kit (Beyotime Institute of Biotechnology; cat. no. P0011). Proteins (30 $\mu$g/lane) were separated using 10% SDS-PAGE and transferred to polyvinylidene fluoride membranes. The membranes were incubated for 2 h with 5% skimmed milk or 5% BSA at room temperature and overnight at 4˚C with primary antibodies against NADPH oxidase (Nox) 2 (cat. no. ab129068; 1:5,000; Abcam), Nox4 (cat. no. ab154244; 1:500; Abcam), Bcl-2 (cat. no. ab194583; 1:500; Abcam), Bax (cat. no. ab182733; 1:2,000; Abcam), cleaved-caspase 3 (cat. no. 9661; 1:500; Cell Signaling Technology, Inc.), caspase 3 (cat. no. ab184787; 1:2,000; Abcam), phosphorylated (p)-JNK (cat. no. ab76572; 1:5,000; Abcam), p-p38 (cat. no. ab4822; 1:1,000; Abcam), JNK (cat. no. ab199380; 1:2,500; Abcam), p38 (cat. no. ab170099; 1:1,000; Abcam), GPX4 (cat. no. ab125066; 1:2,000; Abcam), ferritin heavy chain (FTH1; cat. no. ab183781; 1:1,000; Abcam), long-chain-fatty-acid-CoA ligase 4 (ACSL4; cat. no. ab155282; 1:10,000; Abcam) or GAPDH (cat. no. ab181602; 1:10,000; Abcam). Subsequently, horseradish peroxidase-conjugated goat anti-rabbit secondary antibody (cat. no. ab97080; 1:5,000; Abcam) was applied to incubate the membranes for an additional 2 h at room temperature. Finally, the visualization of the protein bands was performed by an enhanced chemiluminescence reagent (Thermo Fisher Scientific, Inc.). ImageJ software (version 1.52v; National Institutes of Health) was used for densitometric analysis.

*Terminal deoxynucleoitidyl-transferase-mediated dUTP nick end labeling (TUNEL)*. With the application of a TUNEL kit (cat. no. C1091; Beyotime Institute of Biotechnology), the effect of butorphanol on $H_2O_2$-induced PC12 apoptosis was assessed. In short, the fixation and permeabilization of PC12 cells on glass slips were carried out with 4% paraformaldehyde at room temperature for 30 min and 0.25% Triton-X 100 at room temperature for 5 min, separately. Subsequently, the cells were labeled with TUNEL reagent at 37˚C in the dark for 60 min. Finally, nuclear labeling was performed using Vectashield mounting medium containing 50 $\mu$g/ml DAPI for nuclear labeling (Vector Laboratories, Inc.) at room temperature for 5 min. The luminescence intensity was controlled in a fluorescent microscope with a set of fluorescein isothiocyanate filters (green spectrum). Lastly, the images of positive apoptotic cells in three random fields per coverslip were captured by a fluorescent microscope (magnification, x200; Olympus Corporation). The number of TUNEL-positive PC12 cells and the total number of cells were counted using Image-Pro Plus 6.0 software (Media Cybernetics). The percentage of TUNEL-positive PC12 cells in the total cells were counted and the average value was calculated.

*Lipid peroxidation*. The detection of the oxidation of polyunsaturated fatty acids in cell samples was performed by assessing thiobarbituric acid-reactive substances (TBARS) produced during the process of lipid peroxidation, which included lipid peroxides and MDA. The determination of TBARS was performed by fluorimetry which used 1,1,3,3-tetramethoxypropane as the standard.

*Measurement of $Fe^{2+}$*. The collected cells were homogenized with phosphate-buffered saline and centrifuged at 13,000 x g for 10 min at 4˚C for the detection of iron concentration. The latter was quantified by an iron colorimetric assay kit (cat. no. K390; BioVision, Inc.).

*Statistical analysis*. All data are demonstrated as mean ± standard deviation utilizing GraphPad Prism 8.0 software (GraphPad Software, Inc.). Each experiment was repeated at least three times. Tukey's post-hoc test and one-way analysis of variance were employed to conduct statistical comparisons. $P<0.05$ was considered to indicate a statistical significance.

## Results

*Effects of butorphanol treatment on the viability of PC12 cells*. To clarify the role of butorphanol in neurodegenerative diseases, the viability of $H_2O_2$-treated or untreated PC12 cells exposed to butorphanol was measured to verify the hypothesis that butorphanol protects against $H_2O_2$-induced viability injury in PC12 cells. CCK-8 was used to investigate the effects

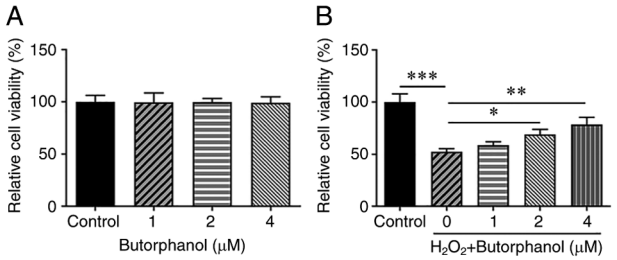


Figure 1. Effects of butorphanol treatment on the viability of PC12 cells. (A) Viability of PC12 cells was detected using the CCK-8 assay. (B) $H_2O_2$-induced PC12 cell viability was detected using the CCK-8 assay. $^{*}P<0.05$, $^{**}P<0.01$, and $^{***}P<0.001$. CCK-8, cell counting kit-8; $H_2O_2$, hydrogen peroxide.

of butorphanol on the viability of PC12 cells as well as on the viability of $H_2O_2$-treated PC12 cells. The viability of PC12 cells remained unchanged following butorphanol treatment (Fig. 1A). However, it was noted that $H_2O_2$ treatment greatly reduced the viability of PC12 cells in comparison with that of the control group (Fig. 1B). Notably, $H_2O_2$-treated PC12 cell viability was gradually reversed with the increasing concentrations of butorphanol, revealing that this compound promoted the viability of $H_2O_2$-exposed PC12 cells in a concentration-dependent manner.

*Butorphanol inhibits oxidative stress in $H_2O_2$-treated PC12 cells*. To explore the role of butorphanol in oxidative stress of $H_2O_2$-treated PC12 cells, the expression levels of oxidative stress factors including MDA, SOD, GSH-Px and CAT were evaluated with the corresponding assay kits to validate the hypothesis that butorphanol may also play a protective role in $H_2O_2$-evoked oxidative stress in PC12 cells. In contrast to the control group, treatment of the cells with $H_2O_2$ significantly increased MDA concentration and significantly decreased SOD, GSH-Px and CAT expression levels. Nevertheless, butorphanol reversed the effects of $H_2O_2$ treatment on the expression of theses markers in a dose-dependent manner, as demonstrated by the decreased MDA concentration as well as the upregulated SOD, GSH-Px and CAT expression levels in comparison with those of the $H_2O_2$ group (Fig. 2A). In addition, the expression levels of oxidative stress-related proteins, including Nox2 and Nox4 were significantly increased in $H_2O_2$-treated PC12 cells, while butorphanol treatment exhibited the opposite effects on these proteins, suggesting that butorphanol imparted suppressive effects on the induction of oxidative stress in $H_2O_2$-treated PC12 cells (Fig. 2B).

*Butorphanol inhibits apoptosis in $H_2O_2$-treated PC12 cells*. The TUNEL assay was used explore the role of butorphanol in $H_2O_2$-induced PC12 apoptosis, and the expression levels of the apoptotic factors were assessed using western blotting to validate the hypothesis that butorphanol may hamper the apoptosis of $H_2O_2$-treated PC12 cells. The significantly increased levels of $H_2O_2$-induced PC12 apoptosis were gradually decreased by butorphanol treatment (Fig. 3A). Notably, butorphanol exhibited inhibitory effects on $H_2O_2$-induced PC12 apoptosis in a dose-dependent manner. In addition, $H_2O_2$ treatment significantly diminished Bcl-2 expression and markedly increased Bax and cleaved-caspase 3 expression, which were subsequently partially reversed by butorphanol treatment, as determined by the upregulated Bcl-2 expression as well as the downregulated Bax and cleaved-caspase 3 expression in $H_2O_2$-treated PC12 cells additionally treated with increasing doses of butorphanol (Fig. 3B). The aforementioned results indicated that butorphanol repressed the apoptosis of $H_2O_2$-treated PC12 cells.

*Butorphanol inhibits ferroptosis by blocking the JNK/p38 signaling pathway*. To examine the latent regulatory mechanism of butorphanol in $H_2O_2$-treated PC12 cells, the results obtained from western blotting indicated that the significantly increased p-JNK and p-p38 expression levels in PC12 cells caused by $H_2O_2$ treatment were gradually decreased following butorphanol administration compared with those of the $H_2O_2$ group (Fig. 4A). Butorphanol (4 $\mu$M) was selected for the remaining experiments. To further identify the mechanism of the JNK/p38 signaling pathway, the JNK activator anisomycin (ANI) was utilized to pre-treat the cells. Increased TBAR levels in $H_2O_2$-treated PC12 cells were subsequently inhibited by butorphanol administration, which was restored by ANI (Fig. 4B).

In addition, butorphanol diminished the increased levels of $Fe^{2+}$ in $H_2O_2$-treated PC12 cells, which were subsequently partially countervailed by ANI administration in comparison with that of the $H_2O_2$ + butorphanol group (Fig. 4C). Moreover, butorphanol treatment downregulated ACSL4 expression and upregulated GPX4 and FTH1 expression levels in $H_2O_2$-treated PC12 cells compared with those noted in the $H_2O_2$ group (Fig. 4D and E). Nevertheless, ANI partially abolished the effects of butorphanol on the expression levels of these ferroptosis-related proteins, as determined by the increased ACSL4 expression and the decreased GPX4 and FTH1 expression in the ANI + $H_2O_2$ + butorphanol group, suggesting that butorphanol inhibited ferroptosis by blocking the JNK/p38 signaling pathway.

*Butorphanol inhibits ferroptosis by blocking the JNK/p38 signaling pathway to suppress oxidative stress in $H_2O_2$-treated PC12 cells*. To further determine whether butorphanol participates in $H_2O_2$-induced PC12 cell oxidative stress by blocking the JNK/p38 signaling pathway and suppressing ferroptosis, the ferroptosis inducer erastin (ERA) was used at a concentration of 30 mM and the JNK activator ANI at a concentration of 10 mM to treat the cells. Following treatment, the oxidative stress levels were detected again. Compared with the $H_2O_2$ + butorphanol group, ANI or ERA treatment significantly enhanced the MDA levels and significantly reduced the levels of SOD, GSH-Px and CAT (Fig. 5A). Furthermore, ANI or ERA administration significantly improved the decreased Nox2 and Nox4 expression levels compared with those noted in the $H_2O_2$ + butorphanol group, indicating that butorphanol inhibited ferroptosis by blocking the JNK/p38 signaling pathway to suppress oxidative stress in $H_2O_2$-treated PC12 cells (Fig. 5B).

*Butorphanol inhibits ferroptosis by blocking the JNK/p38 signaling pathway to suppress $H_2O_2$-induced PC12 apoptosis*. To further determine whether butorphanol participates in $H_2O_2$-induced PC12 apoptosis by blocking the JNK/p38 signaling pathway and suppressing ferroptosis, the apoptosis

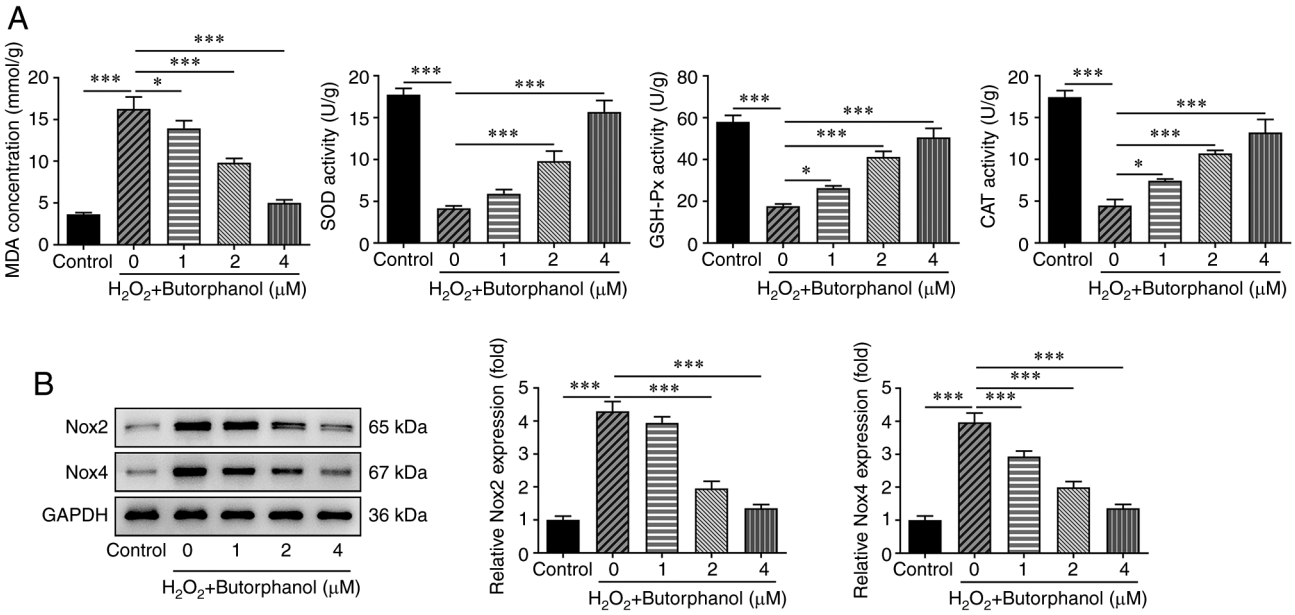


Figure 2. Butorphanol inhibits oxidative stress in $H_2O_2$-treated PC12 cells. (A) Levels of MDA, SOD, GSH-Px and CAT were detected using the corresponding assay kits. (B) Expression levels of the oxidative stress-related proteins were detected using western blotting. $^{*}$P<0.05 and $^{***}$P<0.001. $H_2O_2$, hydrogen peroxide; MDA, malondialdehyde; SOD, superoxide dismutase; GSH-Px, glutathione peroxidase; CAT, catalase.

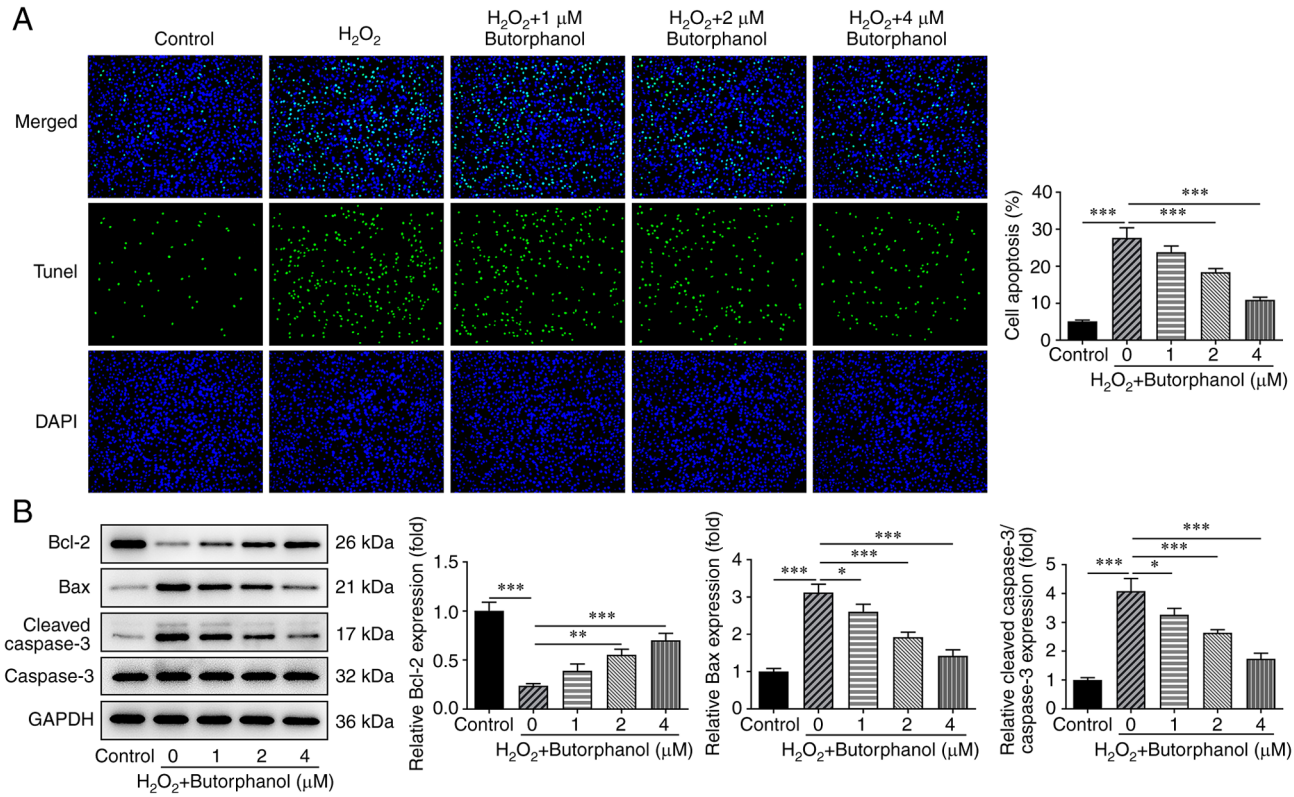


Figure 3. Butorphanol inhibits apoptosis in $H_2O_2$-treated PC12 cells. (A) Induction of apoptosis was detected using the TUNEL assay (magnification, x200). (B) Expression levels of the apoptosis-related proteins were detected using western blotting. $^{*}$P<0.05, $^{**}$P<0.01 and $^{***}$P<0.001. $H_2O_2$, hydrogen peroxide; TUNEL, terminal-deoxynucleoitidyl transferase mediated nick end labeling.

levels were detected again following the addition of ERA and ANI. The results indicated that $H_2O_2$ treatment increased the induction of apoptosis of PC12 cells compared with the control group, which was significantly reduced by butorphanol treatment (Fig. 6A). Evidently, ANI or ERA markedly enhanced the apoptosis of butorphanol-treated PC12 cells exposed to $H_2O_2$ compared with the $H_2O_2$ + butorphanol group. Moreover, treatment of the cells with $H_2O_2$ decreased Bcl-2 levels and increased the levels of Bax and cleaved-caspase 3, which were subsequently reversed by butorphanol, as determined by the

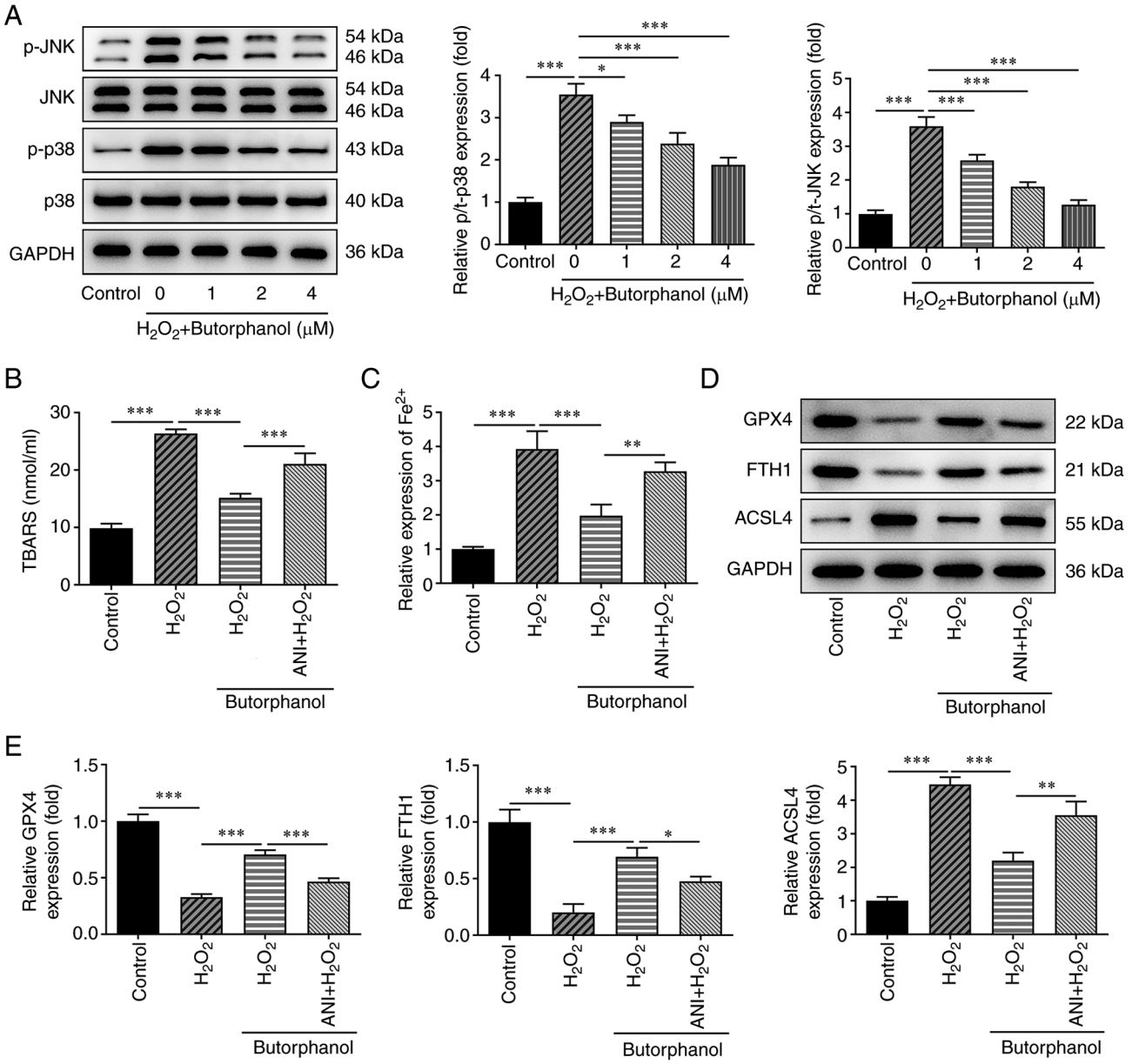


Figure 4. Butorphanol inhibits ferroptosis by blocking the JNK/p38 signaling pathway. (A) Expression levels of the JNK/p38 signaling pathway-related proteins were detected using western blotting. (B) Expression levels of TBARS were detected using the corresponding assay kit. (C) Levels of $Fe^{2+}$ were detected using the iron colorimetric assay kit. (D and E) The expression levels of the ferroptosis-related proteins were detected using western blotting analysis. $^{*}$P<0.05, $^{**}$P<0.01 and $^{***}$P<0.001. JNK, c-Jun NH2-terminal kinase; TBARS, thiobarbituric acid-reactive substances; p-, phosphorylated; t-, total; $H_2O_2$, hydrogen peroxide; FTH1, ferritin heavy chain 1; ACSL4, long-chain-fatty-acid-CoA ligase 4.

enhanced Bcl-2 expression as well as the reduced Bax and cleaved-caspase 3 expression levels in the $H_2O_2$ + butorphanol group (Fig. 6B). Nevertheless, it was noted that the simultaneous addition of ANI and ERA inhibited Bcl-2 levels and promoted the levels of Bax and cleaved-caspase 3 compared with those noted in the $H_2O_2$ + butorphanol group, implying that butorphanol inhibited ferroptosis by blocking the JNK/p38 signaling pathway to suppress $H_2O_2$-induced PC12 apoptosis.

## Discussion

In the present study, $H_2O_2$ was incubated with PC12 cells so as to establish a model of neurodegenerative damage *in vitro*. Through a series of functional experiments, it was revealed that butorphanol suppressed the induction of oxidative stress, apoptosis and ferroptosis of $H_2O_2$-treated PC12 cells. In addition, subsequent experiments demonstrated that butorphanol inhibited ferroptosis by blocking the JNK/p38 signaling pathway to suppress oxidative stress and apoptosis in $H_2O_2$-treated PC12 cells. To the best of our knowledge, this is the first study to preliminarily clarify the possible suppressive role of butorphanol in neurodegenerative diseases as well as its close relation with the JNK/p38 signaling pathway in neurodegenerative diseases.

Neurodegenerative diseases are sporadic and rare hereditary disorders of the central nervous system, which can contribute to the slow progressive loss of the functions of specific neuron populations and their connections (19). Apoptosis is one of the

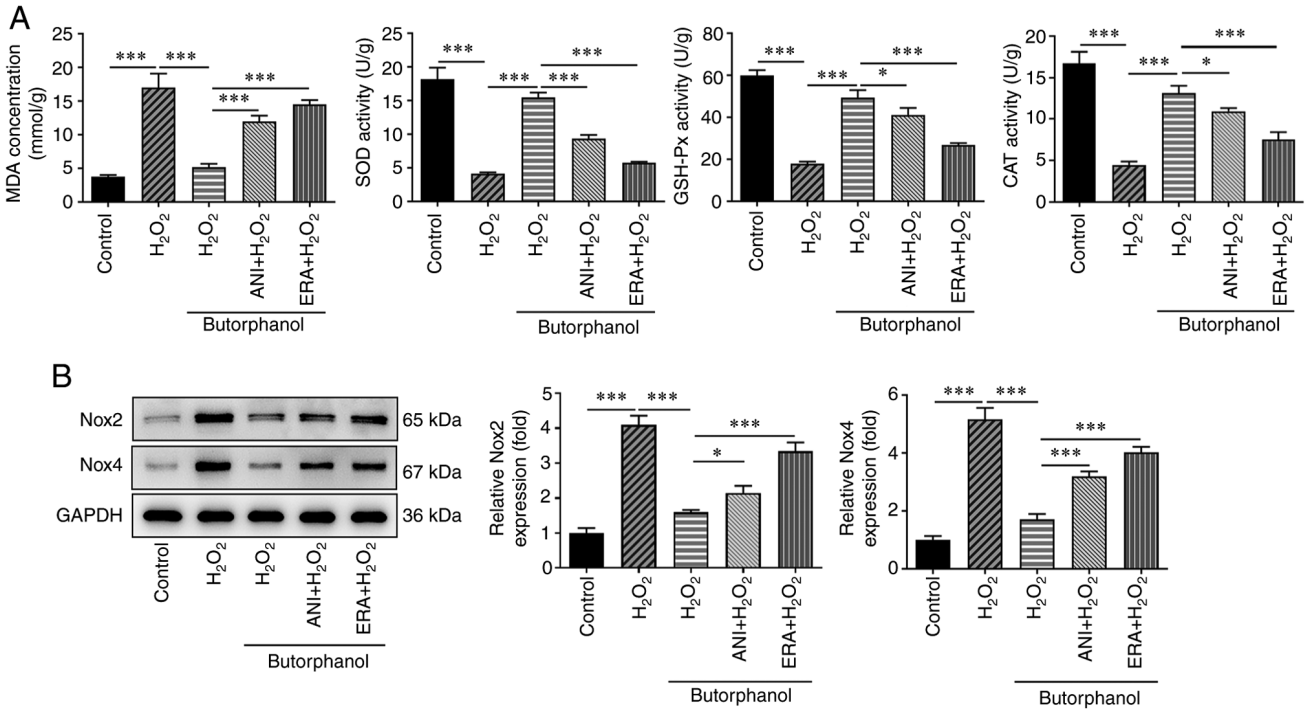


Figure 5. Butorphanol inhibits ferroptosis by blocking the JNK/p38 signaling pathway to suppress oxidative stress in $H_2O_2$-treated PC12 cells. (A) Levels of MDA, SOD, GSH-Px and CAT were detected using the corresponding assay kits. (B) Expression levels of the oxidative stress-related proteins were detected using western blotting. $^{*}$P<0.05 and $^{***}$P<0.001. JNK, c-Jun NH2-terminal kinase; $H_2O_2$, hydrogen peroxide; MDA, malondialhedyde; SOD, superoxide dismutase; GSH-Px, glutathione peroxidase; CAT, catalase; Nox, NADPH oxidase; ANI, anisomycin; ERA, erastin.

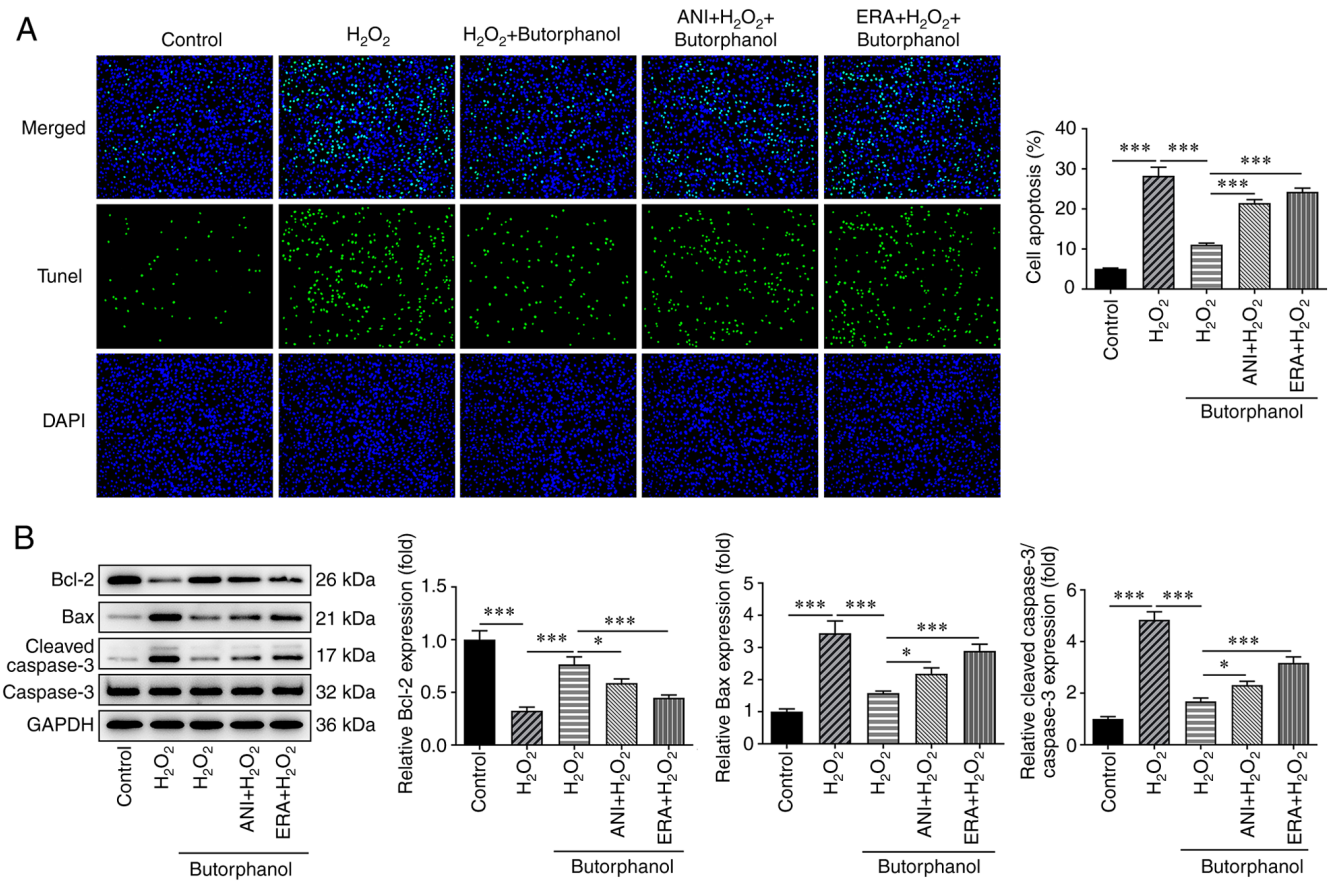


Figure 6. Butorphanol inhibits ferroptosis by blocking the JNK/p38 signaling pathway to suppress apoptosis in $H_2O_2$-treated PC12 cells. (A) Induction of apoptosis was detected using the TUNEL assay (magnification, x200). (B) Expression levels of the apoptosis-related proteins were detected using western blotting. $^{*}$P<0.05 and $^{***}$P<0.001. JNK, c-Jun NH2-terminal kinase; $H_2O_2$, hydrogen peroxide; TUNEL, terminal deoxynucleotidyl-transferase-mediated dUTP nick end labeling; ANI, anisomycin; ERA, erastin.

mechanisms triggering neurodegenerative diseases, during the process of which the apoptotic rate is enhanced and the neural damage may be evident (20). A previous study has demonstrated that anti-apoptotic drugs can alter the apoptotic pathway in neurodegenerative diseases as well as delay the disease progression (21). In addition, it is commonly acknowledged that oxidative stress is a major regulatory element in neurodegenerative diseases (22). Furthermore, ferroptosis has been reported to participate in the apoptosis and neuronal cell damage in PC12 cells (23). Furthermore, butorphanol, a synthetic selective opioid receptor antagonist, has been shown to attenuate apoptosis and oxidative damage in neuronal PC12 cells in recent studies (3,24). In the present study, butorphanol had no influence on the viability of PC12 cells, whereas it markedly decreased $H_2O_2$-induced PC12 cell viability loss, indicating that it could inhibit neuron cell viability loss in a neurodegenerative disease cell model. Moreover, it was also found that the increased Nox2 and Nox4 expressions caused by $H_2O_2$ treatment were markedly reduced by butorphanol treatment, which revealed the inhibitory effects of butorphanol on oxidative stress in neurodegenerative diseases. Furthermore, butorphanol suppressed $H_2O_2$-induced apoptosis in PC12 cells and downregulated the expression levels of the pro-apoptotic proteins Bax and cleaved-caspase 3, suggesting its suppressive effects on the induction of neuronal apoptosis in neurons.

The JNK/p38 signaling pathway is a critical signal transduction pathway that participates in several physiological and pathological responses, such as apoptosis, proliferation and oxidative stress (25,26). The accumulation of $H_2O_2$ has been shown to activate JNK/p38 MAPK signaling in neuronal cells (27). It has also been shown that butorphanol can block p38 and JNK phosphorylation (28). Ferroptosis plays a critical role in neuronal death and neurological disorders. Concomitantly, iron depositions can be detected in specific brain regions of cases with neurodegenerative diseases (7). A previous study suggested that ferroptosis could be regulated by the Ras-JNK/p38 signaling pathway (16). In the present study, butorphanol markedly reduced the expression levels of p-JNK and p-p38 in $H_2O_2$-treated PC12 cells, indicating that it could block the JNK/p38 signaling pathway, which was consistent with the results mentioned in a previous study (28). Moreover, butorphanol diminished the levels of $Fe^{2+}$ and ACSL4 in $H_2O_2$-treated PC12 cells, which were subsequently reversed by treatment with the JNK activator ANI, suggesting that it could suppress ferroptosis by blocking the JNK/p38 signaling pathway.

In order to further assess the relationship among ferroptosis, oxidative stress, apoptosis and the JNK/p38 signaling pathway, the ferroptosis inducer ERA was used to track the effects of the inhibition of ferroptosis caused by the butorphanol-induced blocking of the JNK/p38 signaling pathway on the induction of apoptosis and oxidative stress in $H_2O_2$-treated PC12 cells. In the present study, it was shown that the decreased levels of MDA, Nox2 and Nox4 in $H_2O_2$-treated PC12 cells caused by butorphanol were increased by ANI or ERA administration, indicating that butorphanol inhibited ferroptosis by blocking the JNK/p38 signaling pathway to suppress oxidative stress in neurons. Furthermore, the increased apoptosis levels and the upregulated Bax and cleaved-caspase 3 expressions caused by ANI or ERA administration could be observed in butorphanol-treated PC12 cells exposed to $H_2O_2$. The aforementioned results implied that butorphanol inhibited ferroptosis by blocking the JNK/p38 signaling pathway, thus repressing oxidative stress and apoptosis in a neurodegenerative disease model.

In conclusion, the present study investigated the role of butorphanol and uncovered the relationship among ferroptosis, oxidative stress, apoptosis and the JNK/p38 signaling pathway in a neurodegenerative disease cell model. The findings may provide new insights for the treatment of neurodegenerative diseases.

**Acknowledgements**

Not applicable.

**Funding**

No funding was received.

**Availability of data and materials**

The datasets used and/or analyzed during the current study are available from the corresponding author on reasonable request.

**Authors' contributions**

LJ, QS, PZ and YQ conceived and designed the study, and acquired and interpreted the data. LJ, QS, PZ and YQ performed the experiments. LJ, QS, PZ and YQ wrote the manuscript. LJ, QS, PZ and YQ confirm the authenticity of all the raw data. All authors have read and approved the final version of the manuscript.

**Ethics approval and consent to participate**

Not applicable.

**Patient consent for publication**

Not applicable.

**Competing interests**

The authors declare that they have no competing interests.

**References**

1. Luan G, Pan F, Bu L, Wu K, Wang A and Xu X: Butorphanol promotes macrophage phenotypic transition to inhibit inflammatory lung injury via κ receptors. Front Immunol 12: 692286, 2021.
2. Jose DE, Ganapathi P, Anish Sharma NG, Shankaranarayana P, Aiyappa DS and Nazim M: Postoperative pain relief with epidural buprenorphine versus epidural butorphanol in laparoscopic hysterectomies: A comparative study. Anesth Essays Res 10: 82-87, 2016.
3. Yang Z, Wang L, Hu Y and Wang F: Butorphanol protects PC12 cells against OGD/R-induced inflammation and apoptosis. Mol Med Rep 22: 1969-1975, 2020.
4. Wang B, Li Y, Shen Y, Xu Y and Zhang C: Butorphanol inhibits the malignant biological behaviors of ovarian cancer cells via down-regulating the expression of TMEFF1. Onco Targets Ther 13: 10973-10981, 2020.

5. Dugger BN and Dickson DW: Pathology of neurodegenerative diseases. Cold Spring Harb Perspect Biol 9: a028035, 2017.
6. Li J, Cao F, Yin HL, Huang ZJ, Lin ZT, Mao N, Sun B and Wang G: Ferroptosis: Past, present and future. Cell Death Dis 11: 88, 2020.
7. Reichert CO, de Freitas FA, Sampaio-Silva J, Rokita-Rosa L, Barros PL, Levy D and Bydlowski SP: Ferroptosis mechanisms involved in neurodegenerative diseases. Int J Mol Sci 21: 8765, 2020.
8. Wang X, Zhao J, Han Z and Tang F: Protective effects of semen crotonis pulveratum on trinitrobenzene sulphonic acid-induced colitis in rats and $H_2O_2$-induced intestinal cell apoptosis *in vitro*. Int J Mol Med 35: 1699-1707, 2015.
9. Cai X, Zhu L, Chen X, Sheng Y, Guo Q, Bao J and Xu J: X/XO or H2O2 induced IPEC-J2 cell as a new in vitro model for studying apoptosis in post-weaning piglets. Cytotechnology 68: 713-724, 2016.
10. Rice ME: H2O2: A dynamic neuromodulator. Neuroscientist 17: 389-406, 2011.
11. Falcicchia C, Tozzi F, Arancio O, Watterson DM and Origlia N: Involvement of p38 MAPK in synaptic function and dysfunction. Int J Mol Sci 21: 5624, 2020.
12. Su AR, Qiu M, Li YL, Xu WT, Song SW, Wang XH, Song HY, Zheng N and Wu ZW: BX-795 inhibits HSV-1 and HSV-2 replication by blocking the JNK/p38 pathways without interfering with PDK1 activity in host cells. Acta Pharmacol Sin 38: 402-414, 2017.
13. Lanna A, Gomes DC, Muller-Durovic B, McDonnell T, Escors D, Gilroy DW, Lee JH, Karin M and Akbar AN: A sestrin-dependent Erk-Jnk-p38 MAPK activation complex inhibits immunity during aging. Nat Immunol 18: 354-363, 2017.
14. Li J, Xu B, Chen Z, Zhou C, Liao L, Qin Y, Yang C, Zhang X, Hu Z, Sun L, *et al*: PI3K/AKT/JNK/p38 signalling pathway-mediated neural apoptosis in the prefrontal cortex of mice is involved in the antidepressant-like effect of pioglitazone. Clin Exp Pharmacol Physiol 45: 525-535, 2018.
15. Wu K, Hu L and Hou J: Selective suppression of Notch1 inhibits proliferation of renal cell carcinoma cells through JNK/p38 pathway. Oncol Rep 35: 2795-2800, 2016.
16. Ye F, Chai W, Xie M, Yang M, Yu Y, Cao L and Yang L: HMGB1 regulates erastin-induced ferroptosis via RAS-JNK/p38 signaling in HL-60/$NRAS^{Q61L}$ cells. Am J Cancer Res 9: 730-739, 2019.
17. Zhang H, Jiao W, Cui H, Sun Q and Fan H: Combined exposure of alumina nanoparticles and chronic stress exacerbates hippocampal neuronal ferroptosis via activating IFN-γ/ASK1/JNK signaling pathway in rats. J Hazard Mater 411: 125179, 2021.
18. Aminzadeh A, Dehpour AR, Safa M, Mirzamohammadi S and Sharifi AM: Investigating the protective effect of lithium against high glucose-induced neurotoxicity in PC12 cells: Involvements of ROS, JNK and P38 MAPKs, and apoptotic mitochondria pathway. Cell Mol Neurobiol 34: 1143-1150, 2014.
19. Reith W: Neurodegenerative diseases. Radiologe 58: 241-258, 2018 (In German).
20. Radi E, Formichi P, Battisti C and Federico A: Apoptosis and oxidative stress in neurodegenerative diseases. J Alzheimers Dis 42 (Suppl 3): S125-S152, 2014.
21. Erekat NS: Apoptosis and its therapeutic implications in neurodegenerative diseases. Clin Anat 35: 65-78, 2022.
22. Singh A, Kukreti R, Saso L and Kukreti S: Oxidative stress: A key modulator in neurodegenerative diseases. Molecules 24: 1583, 2019.
23. Wu C, Zhao W, Yu J, Li S, Lin L and Chen X: Induction of ferroptosis and mitochondrial dysfunction by oxidative stress in PC12 cells. Sci Rep 8: 574, 2018.
24. Tsukamoto A, Iimuro M, Sato R, Yamazaki J and Inomata T: Effect of midazolam and butorphanol premedication on inhalant isoflurane anesthesia in mice. Exp Anim 64: 139-145, 2015.
25. Bu X, Xia W, Wang X, Lu S and Gao Y: Butylphthalide inhibits nerve cell apoptosis in cerebral infarction rats via the JNK/p38 MAPK signaling pathway. Exp Ther Med 21: 565, 2021.
26. Lv WP, Li MX and Wang L: Peroxiredoxin 1 inhibits lipopolysaccharide-induced oxidative stress in lung tissue by regulating P38/JNK signaling pathway. Eur Rev Med Pharmacol Sci 21: 1876-1883, 2017.
27. Li WW, Gao XM, Wang XM, Guo H and Zhang BL: Icariin inhibits hydrogen peroxide-induced toxicity through inhibition of phosphorylation of JNK/p38 MAPK and p53 activity. Mutat Res 708: 1-10, 2011.
28. Huang LH, Li J, Gu JP, Qu MX, Yu J and Wang ZY: Butorphanol attenuates myocardial ischemia reperfusion injury through inhibiting mitochondria-mediated apoptosis in mice. Eur Rev Med Pharmacol Sci 22: 1819-1824, 2018.